Application of a transient-hot-electron-transport Green's-function approach to a two-dimensional model of a GaAs/$Al_xGa_{1-x}As$ heterojunction

Javier E. Hasbun
Department of Physics, West Georgia College, Carrollton, Georgia 30118

Tsu W. Nee
Michelson Laboratory, Physics Division, Naval Weapons Center, China Lake, California 93555
(Received 25 June 1990; revised manuscript received 27 February 1991)

The Green's-function approach to transient-hot-electron transport of Xing and Ting [Phys. Rev. B **35**, 3971 (1987)] is applied to a GaAs/$Al_xGa_{1-x}As$ heterojunction. Scattering mechanisms, such as remote and background ionized impurity scattering as well as acoustic (via deformation potential and piezoelectric coupling) and polar-optical-phonon contributions, have been included in the force and energy transient state equations. The effect of screening on the ionized impurities by the free carriers has been taken into account approximately. Our results for the transient velocity are in reasonable agreement with available Monte Carlo simulations. Theoretical calculations for the transient velocity and electron temperature have been carried out for electrons with and without electron-electron interactions.

I. INTRODUCTION

Understanding the transient behavior of electrons in a heterojunction under high electric fields is of great importance in the physics of small devices. Electrons in modulation-doped heterostructures grown by molecular-beam epitaxy[1] can achieve high velocities. Mobilities approaching 10^6 $cm^2/V\,s$ in the dark[2] and even higher[3] at low temperatures have been reported.

In short channel GaAs/$Al_xGa_{1-x}As$ heterojunction devices the electron relaxation length is of the order of the distance in which the electric field changes significantly; therefore, as the size of the device gets smaller it becomes increasingly important to have a knowledge of the scattering mechanisms as well as electrons' transient velocity and temperature during their flight through the two-dimensional channel parallel to the heterojunction interface.

Hot-electron effects in semiconductor devices have been the subject of much interest for the past three decades.[4,5] There exists a number of works proposed to deal with transient transport, but most realistic calculations have been based on the phenomenological Boltzmann equation[6] and the Monte Carlo method.[7]

A non-Boltzmann approach to hot electronic transport has recently appeared in the literature. This work is based on the study of the nonlinear steady-state electron transport for a system of electrons interacting with impurities and phonons by Lei and Ting.[8,9] This is an analytical Green's-function approach to high-field transport which is based on the separation of the center-of-mass motion from the relative motion of the electrons in the Hamiltonian[10] and the density matrix.

More recently Xing and Ting[11] extended the above Green's-function formalism to study the transient current due to hot electrons after turning on a strong electric field. Here, as in the above works,[8-10] the statistical properties of the relative electrons are described by the standard many-body theory. In addition, these electrons are coupled with the electric field via the electron-impurity and electron-phonon interactions.

The basic idea of the above approach[11] is that the evolution equation describing the current density or center-of-mass velocity $V(t)$ is coupled with the evolution equation for the electron temperature $T_e(t)$. The differential equation for $V(t)$ includes a term which is proportional to the electric field, which increases it, and terms which include the scattering mechanisms due to ionized impurity (remote and background) and phonons (acoustic and optical), which decrease it. The differential equation that describes $T_e(t)$ has terms such as the energy input due to the electric field, the kinetic energy of the center of mass, and the energy lost to the phonon system. Finally, the above equations are to be solved self-consistently for $V(t)$ and $T_e(t)$.

In this paper we make use of the versatility of this method[11] to study the transient transport of a two-dimensional electron gas (2DEG) parallel to a GaAs/$Al_xGa_{1-x}As$ heterojunction interface in the electric quantum limit. In Sec. II we present the model Hamiltonian which includes contributions due to impurities and phonons. We also give in this section the two-dimensional coupled equations for $V(t)$ and $T_e(t)$. In Sec. III we specialize to the electric quantum limit. In Sec. IV, we present our results, followed by our conclusion in Sec. V.

II. MODEL HAMILTONIAN

A. Contributions due to impurities and phonons

We work with the Hamiltonian for a 2DEG in a GaAs/$Al_xGa_{1-x}As$ heterojunction in the presence of im-

purities, phonons, and an electric field parallel to the interface given by[12]

$$H = H_c + H_e + H_{\text{ph}} + H_{e\text{-}i} + H_{e\text{-ph}} , \tag{2.1}$$

where H_c is the contribution due to the center-of-mass part given by

$$H_c \equiv \frac{P^2}{2Nm} - eNER , \tag{2.2}$$

and describes the coupling of the electric field with the center-of-mass coordinates in the x and y directions defined as

$$\mathbf{P} = \sum_i \mathbf{p}_i , \quad \mathbf{R} \equiv \frac{1}{N} \sum_i \mathbf{r}_i . \tag{2.3a}$$

Here $\mathbf{P} \equiv (P_x, P_y)$, $\mathbf{R} \equiv (R_x, R_y)$, and N is the number of electrons in the conduction channel. The quantities $\mathbf{p}_i \equiv (p_{xi}, p_{yi})$ and $\mathbf{r}_i \equiv (x_i, y_i)$ are the relative momentum and coordinate of the ith electron along the interface which are given in terms of the center-of-mass coordinates by

$$\mathbf{p}_i' = \mathbf{p}_i - \frac{\mathbf{P}}{N} , \quad \mathbf{r}_i' = \mathbf{r}_i - \mathbf{R} . \tag{2.3b}$$

With the above notation the rest of the terms in the total Hamiltonian, i.e., the relative electron H_e, the phonon H_{ph}, the electron-impurity $H_{e\text{-}i}$, and the electron-phonon $H_{e\text{-ph}}$ interactions, are given in second quantized form in Ref. 12. It is important to note here, however, that while the electric field appears to couple only the center-of-mass coordinates in Eq. (2.2), in actuality the relative electron coordinates are coupled to the electric field through the electron-impurity and electron-phonon interactions $H_{e\text{-}i}$ and $H_{e\text{-ph}}$, respectively.

In the above Hamiltonian the electron states are characterized by a subband index n and a two-dimensional wave vector $\mathbf{k} \equiv (k_x, k_y)$ with wave function ψ_{nk} and subband energy E_{nk} given by

$$\begin{aligned} \psi_{nk}(r,z) &= (1/A)^{1/2} \exp[i(kr)] \zeta_n(z) , \\ E_{nk} &= E_n + \frac{\hbar^2 k^2}{2m} , \end{aligned} \tag{2.4}$$

where $\zeta_n(z)$ is the envelope wave function which describes the quantized motion in the z direction with associated energy E_n, and A is the area of the sample. The matrix elements in the total Hamiltonian make use of the above wave function and are given in Ref. 12.

B. Nonlinear equations of transient transport

In the recent work of Xing and Ting[11] a Green's-function approach to transient-hot-electron transport in semiconductors was developed. Here coupled differential equations for the evolution of the drift velocity $V(t)$ and the electron temperature $T_e(t)$ were obtained. Regarding the drift velocity, the authors studied a linearized Langevin equation for $V(t)$ as a function of t. Equation (35) of that work[11] reads

$$\frac{d}{dt} V(t) = \frac{eE}{m} \varphi(t) + \int_0^t k(t, t-s) V(t,s) ds$$

for the transient velocity. Here $\varphi(t)$ is a step function defined below. The kernel $k(t, t-s)$ carries information on the different scattering mechanisms (i.e., impurities and phonons). The second term of $V(t)$ in the above equation depends on its previous values $V(t,s)$; that is, its memory. Furthermore, it is possible to obtain an equation for $V(t)$ where all the above memory effects are contained in the memory function $M(t,\omega)$.

The memory function thus obtained, however, depends on time and frequency in addition to being computationally involved. Nevertheless, by replacing the memory function by its value at $\omega = 0$, the authors[11] obtained a $V(t)$ appropriate for moderate field values in the form

$$V(t) = \frac{eE}{m} \int_0^t ds \exp\left[\int_s^t M_2(u,0) du \right] , \tag{2.5}$$

where $M_2(u,\omega)$ is the imaginary part of the memory function at time u and frequency ω given below.

The above neglect of the frequency dependence on $M(t,\omega)$ corresponds to neglecting the frequency dependence in the electron's scattering lifetime $\tau(t) \equiv [M_2(t,0)]^{-1}$; thus τ is time dependent through the coupling between $V(t)$ and $T_e(t)$. In this manner nonlinear effects are also included.

The imaginary part of the memory function above includes contributions to the scattering experienced by the electrons due to remote and background ionized impurities and phonons. For the case of the 2DEG in the $GaAs/Al_xGa_{1-x}As$ heterojunction case studied here at temperature T and including the multisubbands, we obtain

$$\begin{aligned} M_2(u,\omega) = \frac{1}{Nm} \sum_{q,n'n} q_x^2 \left[\int n_i(z_0) |u_{nn'}(q,z_0)|^2 dz_0 \right] [\Pi_2(nn',q,z) - \Pi_2(nn',q,0)]/\omega \\ + \frac{1}{Nm} \sum_{q,q_z,\lambda,n,n'} |M_{n,n'}(q,q_z,\lambda)|^2 \frac{q_x^2}{\omega} \left\{ \left[n\left[\frac{\hbar\Omega_{Q\lambda}}{k_B T} \right] - n\left[\frac{\hbar(\Omega_{Q\lambda}+\omega)}{k_B T_e} \right] \right] \Pi_2(nn',q,\Omega_{Q\lambda}+\omega) \right. \\ \left. - \left[n\left[\frac{\hbar\Omega_{Q\lambda}}{k_B T} \right] - n\left[\frac{\hbar(\Omega_{Q\lambda}-\omega)}{k_B T_e} \right] \right] \Pi_2(nn',q,\Omega_{Q\lambda}-\omega) \right\} , \end{aligned} \tag{2.6}$$

where

$$n(x)=[\exp(x)-1]^{-1}, \quad Q\equiv(q,q_z), \quad q\equiv(q_x,q_y) . \tag{2.7}$$

The unscreened electron-impurity interaction matrix element for an impurity located at (r_a,z_a) is given by

$$u_{nn'}(q,z_a)=\frac{Ze^2}{2\epsilon Aq}F_{nn'}(q,z_a) , \tag{2.8a}$$

and the electron-phonon interaction matrix elements for the λth branch are given by

$$M_{nn'}(q,q_z,\lambda)=M(q,q_z,\lambda)I^*_{nn'}(iq_z) , \tag{2.8b}$$

with $M(q,q_z,\lambda)$ the electron-phonon interaction strength in a three-dimensional plane-wave representation.

In Eq. (2.6) $\Omega_{q\lambda}$ is the phonon-dispersion relation for the λth branch, Π_2 is the imaginary part of the density-density correlation Green's function Π, which is given in Ref. 12 along with the expressions for F_{nn} and $I_{nn'}$ of Eqs. (2.8). We note that the electron-electron interactions of the 2DEG can be included (e-e), within the random-phase approximation (RPA), or excluded (no e-e) in a straightforward manner through the function Π of Eq. (2.6).

While not immediately obvious from Eq. (2.6), the memory function $M_2(u,\omega)$ is an implicit function of time through the time-dependent electron temperature $T_e(t)$. The differential equation obeyed by $T_e(t)$ has been obtained under the same conditions as the linearized Langevin equation for $V(t)$ above[11] without any further approximations. It is given by[11]

$$C_e\frac{d}{dt}T_e=NeEV(t)\varphi(t)-NmV(t)\frac{d}{dt}V(t)-W(T_e) , \tag{2.9}$$

where C_e is the electronic specific heat[13] in the absence of electron-electron interactions, and given here by

$$C_e=\frac{\partial}{\partial T_e}\left[\sum_{n,k}E_{nk}f(E_{nk})\right] , \tag{2.10}$$

and $\varphi(t)$ is a step function which is unity for $t>0$ (otherwise it is zero), $f(E_{nk})$ is the Fermi function, and $T_e=T$ at $t=0$.

In the above equation for T_e, the first term corresponds to the rate of energy input due to the applied field E, and the second is the rate of change of kinetic energy of the center of mass. The third term $W(T_e)$ carries information on the rate of energy loss of the relative electrons to the phonons. It is given here by

$$W(T_e)=2\sum_{q,q_z,\lambda,nn'}|M_{nn'}(q,q_z,\lambda)|^2\Omega_{Q\lambda}\Pi_2(nn',q,\Omega_{Q\lambda}) \times\left[n\left[\frac{\hbar\Omega_{Q\lambda}}{k_BT}\right]-n\left[\frac{\hbar(\Omega_{Q\lambda})}{k_BT_e}\right]\right] , \tag{2.11}$$

with the notion that in the above equations $V(t)$ and $T_e(t)$ constitute a coupled set of nonlinear equations.

Finally, it should be mentioned here that in general an electric field is viewed as low ($0\lesssim E\lesssim 0.5$ kV/cm) when nonlinear effects (such as overshoot, hot-electron transport, etc.) in $V(t)$ do not play an important role. Such a situation warrants a linear transport theory. If the field reaches a value for which nonlinear effects play an important role in transport, this field is viewed as moderate ($0.5\lesssim E\lesssim 2$ kV/cm) or strong ($E\gtrsim 2$ kV/cm), depending on the prominence of the nonlinear effects.[11,14]

The present approximation employed in our work here is appropriate for fields of moderate strengths because of the approximations made in deriving them.[11] However, a set of equations applicable to strong fields has also been obtained by these authors which have not been investigated thus far for transient transport in heterojunctions.

III. ELECTRIC QUANTUM LIMIT

We now specialize to the case for which the lowest subband is populated in the GaAs/$Ga_xAl_{1-x}As$ heterojunction. In this limit we neglect upper subband effects and the above equations of Sec. II are greatly simplified. We take $n=n'\equiv 0$ in the expressions of Eqs. (2.6)–(2.11). Furthermore, for the lowest subband we make use of the variational envelope wave function[15]

$$\zeta(z)=\left[\frac{b^3}{2}\right]^{1/2}ze^{-bz/2} , \tag{3.1a}$$

where b is a variational parameter determined by minimization of the total energy given by[16]

$$b^3=\frac{12m_ze^2}{\hbar^2\epsilon}(N_{\rm depl}+\tfrac{11}{32}N_s) , \tag{3.1b}$$

where $N_{\rm depl}$ and N_s are the depletion layer and interface carrier density, respectively. The density-density correlation function Π_2 of Eqs. (2.6) and (2.11) is the imaginary part of Π, which is given within the RPA by

$$\Pi(00,q,w)\rightarrow\Pi(q,w)=\frac{\Pi_0(q,w)}{1-V(q)\Pi_0(q,w)} , \tag{3.2}$$

where $V(q)$ is the electron-electron scattering potential (e-e) given by

$$V(q)=\frac{e^2}{2A\epsilon q}H(q) , \tag{3.3a}$$

$$H(q)=\frac{1}{8(b+q)^3}(8b^3+9b^2q+3bq^2) . \tag{3.3b}$$

The unscreened ionized impurity scattering contribution to Eq. (2.6) with the use of Eq. (2.8a) is given by[12]

$$\int n_i(z_0)|u(q,z_0)|^2dz_0 =\left[\frac{Ze^2}{2\epsilon Aq}\right]^2[AN_II(q)^2e^{-2qs}+An_iJ(q)] , \tag{3.4a}$$

where

$$I(q)=\frac{b^3}{(q+b)^3} \tag{3.4b}$$

and

$$J(q)=\frac{1}{4(b+q)^6q}(2b^6+24b^5q+48b^4q^2+43b^3q^3+18b^2q^4+3bq^5)\ . \quad (3.4c)$$

In the present work we include phonon-scattering contributions in Eqs. (2.6) and (2.11) from acoustic (via deformation potential and piezoelectric coupling) and polar-optical (via Frolich coupling) phonons. The form of these terms is given in Ref. 12. The value of the phonon constants used here are given in Table I.

We have recently carried out a study of transient transport in a GaAs/$Al_xGa_{1-x}As$ heterojunction.[17] In this work we made use of a linear theory approach[18] and investigated the above unscreened impurity scattering contribution. We found that the transient velocity versus time curve obtained was much smaller than a Monte Carlo result[19] for $E=1$ kV/cm for the case when the electron-electron interactions were not included (no e-e). We have found that the reason for the discrepancy was due to the neglect of ionized impurity screening.[17] In the present work, the effects of screened ionized impurity scattering can be taken into account in an approximate way.

In the recent Monte Carlo work[19] the authors obtained an expression for the initial guess of the self-consistent screened ionized impurity potential which in the present limit becomes

$$\varphi(q,z,z_0)=-\frac{1}{q}e^{-q|z-z_1|}S_1\frac{Ze^2e^{-q|z_1-z_0|}}{2\epsilon A(q+S_1)}+\frac{Ze^2}{2\epsilon qA}e^{-q|z-z_0|} \quad (3.5)$$

for an impurity at z_0 away from the heterojunction interface. Here z_1 is the position of the maximum value of the ground-state wave function in the interface, and S_1 is given below. If we make the approximation

$$e^{-q|z-z_1|}e^{-q|z_1-z_0|}\simeq e^{-q|z-z_0|} \quad (3.6)$$

in Eq. (3.5), we obtain an approximate expression for $u(q,z)$ to include screening given by

$$u(q,z_a)=\int\varphi(q,z,z_a)|\zeta(z)|^2dz=\frac{Ze^2}{2\epsilon A(q+\lambda S_1)}F_{00}(q,z_a)\ . \quad (3.7)$$

Here λ is to be considered a parameter. A value of $\lambda=0$ implies a complete neglect of screening [Eq. (2.8a)], and $\lambda=1$ corresponds to the above approximation. The quantity S_1 above is given by

TABLE I. Parameters used throughout our calculations of Figs. 1–4.

Quantity	Description	Value
A	Sample area	1 cm^2
d_a	$Al_xGa_{1-x}As$ doped layer thickness	400 Å
$N_i=(N_D-N_A)d_a$	Areal impurity density in the alloy side	2.0×10^{12} cm^{-2}
n_i	Background impurity density	1×10^{15} cm^{-3}
K,K_∞	GaAs and optical dielectric constants	12.9, 10.92
m	Effective mass	$0.067m_0$
N_s	Areal carrier density	5×10^{11} cm^{-2}
N_{depl}	Depletion charge density	5×10^{10} cm^{-2}
N_{depl}	Depletion charge density	cm^{-2}
s	Spacer layer thickness	100 Å
τ_b	Time unit	1.20×10^{-13} sec
T_b	Temperature unit	63.575 K
γ,W_0	Units of M_2 and W	8.32×10^{12} Hz, 731 W
E	Electric field	0.5, 1, 2, 3 kV/cm
T	Lattice temperature	77 K
b_0	Subband parameter	3.20×10^6 cm^{-1}
E_0	Subband energy	$\equiv0$ meV
E_{fo}	$T=0$ Fermi energy	17.89 meV
v_{sl},v_{st}	Transverse, longitudinal sound speed	5.24, 2.48 (10^5 cm/sec)
d	Crytal mass density	5.36 g/cm^3
Ω_0	Optical-phonon frequency	5.38×10^{13} Hz
σ	Deformation potential	7 eV
e_{14}	Piezoelectric constant	1.2×10^9 V/m

$$S_1=\frac{e^2N}{2\epsilon AE_{d_1}},$$

$$E_{d_1}=k_BT_e\left[1+\exp\left[-\frac{E_F-E_0}{k_BT_e}\right]\right]\times\ln\left[1+\exp\left[\frac{E_F-E_0}{k_BT_e}\right]\right], \tag{3.8}$$

where E_F is the electron-temperature-dependent Fermi energy given by

$$E_F(T_e)=E_0+k_BT_e\ln\left[\exp\left[\frac{E_F(0)}{k_BT_e}\right]-1\right],$$
$$E_F(0)=E_0+\frac{\pi N_s\hbar^2}{m}, \tag{3.9}$$

obtained from $N=2\sum_k f(E_k)$. Here $E_F(0)$ is the $T_e=0$ Fermi energy, and we also take $E_0\equiv 0$. The electronic specific heat in the present limit is given by

$$C_e=\frac{mA}{\pi\hbar^2}\left[E_F(T_e)\frac{\partial}{\partial T_e}E_F(T_e)+\frac{\pi^3}{3}k_B^2T_e\right], \tag{3.10}$$

which has been obtained from Eq. (2.10).

Finally, we note that the parameter λ above has a distant relationship with the self-consistent screened impurity potential of Yokoyama and Hess.[19] That is, $\lambda=1$ corresponds to the neglect of impurity Green's-function correlations [Eq. (3.6)] in the first guess of the self-consistent screened impurity potential. Thus we treat λ as an interpolating parameter between $\lambda=0$ (no screening) and $\lambda=1$.

IV. RESULTS

In this section our numerical results of the nonlinear equations (2.5) and (2.9) for moderate electric-field strengths are presented. Scattering mechanisms such as impurities and phonons (acoustic and optical) have been included. The calculations have been carried out in the presence of electron-electron interactions (e-e) and in their absence (no e-e). The values of the parameters used throughout are given in Table I. In this table $\tau_b\equiv\hbar/E_b$, $T_b\equiv E_b/k_B$, $\gamma\equiv\tau_b^{-1}$, and $W_0\equiv(E_b/\tau_b)\times 10^{11}$, where $E_b\equiv me^4/2\hbar^2(4\pi\epsilon)^2$. Here m is the GaAs effective mass, k_B is Boltzmann's constant, and $\epsilon=K\epsilon_0$ is the GaAs dielectric constant.

Here a comparison between this theory and a Monte Carlo (MC) method would be helpful in order to see the differences between the two methods for describing transient transport. The present method, in contrast to the MC works, is an analytical quantum-mechanical many-body approach which requires less numerical effort than a Monte Carlo calculation.

In Fig. 1 we compare our results for the transient velocity [Eqs. (2.5)–(2.9)] with a MC simulation[19] for the case of no e-e. In this figure we show that our $V(t)$ is in reasonable agreement with the MC results when the ionized impurity screening parameter $\lambda=0.5$. As the value of λ increases, the impurity screening increases in strength, thus lowering the impurity scattering and increasing the overall value of the velocity. The agreement for $\lambda=0.5$ is best at longer times since we expect that in the limit of very large times the electrons reach equilibrium conditions and can be described classically. In this

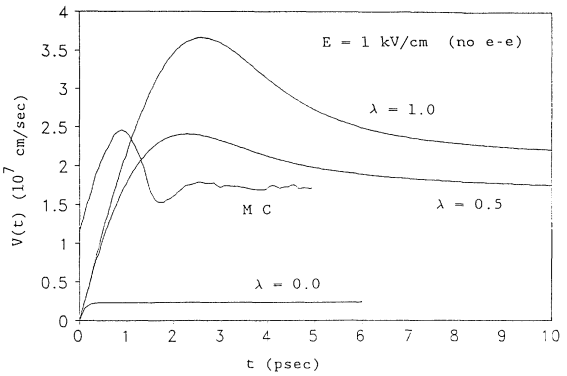

FIG. 1. Comparison of $V(t)$ vs t with the Monte Carlo simulation of Ref. 19 for $E=1$ kV/cm in the absence of e-e interactions. $\lambda=0$ is the nonscreened ionized impurity scattering.

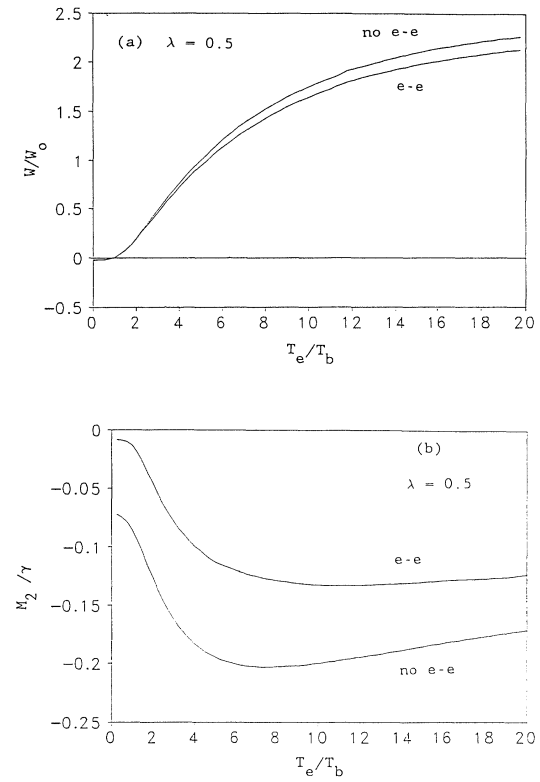

FIG. 2. (a) The calculated energy-loss rate of electrons W/W_0 as a function of T_e/T_b for the cases of e-e and no e-e with acoustic and optical phonons. (b) The calculated scattering rate of electrons M_2/γ as a function of T_e/T_b for e-e and no e-e. Screened ionized impurity scattering ($\lambda=0.5$) in addition to phonons has been included.

limit both approaches give the same results.

The case for which $\lambda=0$ includes no screening resulting in a small value of the velocity and no overshoot behavior. The rest of the calculations have been carried out for a value of $\lambda=0.5$.

In Fig. 2(a) we show our results for the calculated rate of electron energy loss to phonons, W [Eq. (2.11) with $n=n'\equiv 0$], in units of W_0 of Table I. Here W is shown as a function of temperature T_e in units of T_b of Table I for both cases of when the electron-electron interactions are included (e-e) and excluded (no e-e). The case of no e-e has a slightly higher energy-loss rate than the e-e case. While W has contributions due to acoustic- and polar-optical phonons, the shape and magnitude of W is largely dominated by its polar-optical-phonon contribution. We note that W is negative below $T=77$ K because when T_e is lower than the lattice temperature T, energy flows from the lattice to the electron system.[20]

In Fig. 2(b) the memory function M_2 (in units of γ of Table I) [Eq. (2.6) with $n=n'\equiv 0$] is plotted versus electron temperature T_e (in units of T_b of Table I). The memory function contains contributions due to screened ionized impurity scattering (remote and background) with $\lambda=0.5$ and contributions due to acoustic- and polar-optical phonons. The magnitude and shape of both (e-e and no e-e) curves are dominated by impurity scattering at electron temperatures lower than about 100 K and by polar-optical phonons for electron temperatures above 100 K. We also see in Fig. 2(b) that the M_2 which includes e-e is smaller in magnitude than the M_2 which excludes e-e due to the many-body screening effects in the e-e case.

The above curves for $W(T_e)$ and $M_2(T_e)$, which are the most time consuming part of the calculations, have been used to obtain the transient properties $V(t)$ and $T_e(t)$.

In Fig. 3 we show the velocity and electron temperature curves for the case of no e-e. The different curves correspond to different values of the applied field. In Fig. 3(a) $V(t)$ is plotted versus time. We see that as the electric field is increased, the magnitude of the velocity is increased, and the overshoot peak shifts to shorter times. In Fig. 3(b) the electron temperature corresponding to each $V(t)$ curve of Fig. 3(a) is shown. The onset of electron heating as a function of time occurs earlier as the electric field is increased. This onset gives rise to the overshoot in the $V(t)$ curves. As the electron temperature increases, so does the scattering mechanisms in M_2 and the rate of energy loss to phonons W as shown in Fig. 2. This results in a decrease in velocity as time progresses until steady state is reached. A slight undershoot is seen for higher fields in Fig. 3(a), which is due to another increase in T_e for $E=3$ kV/cm. However, in this regime

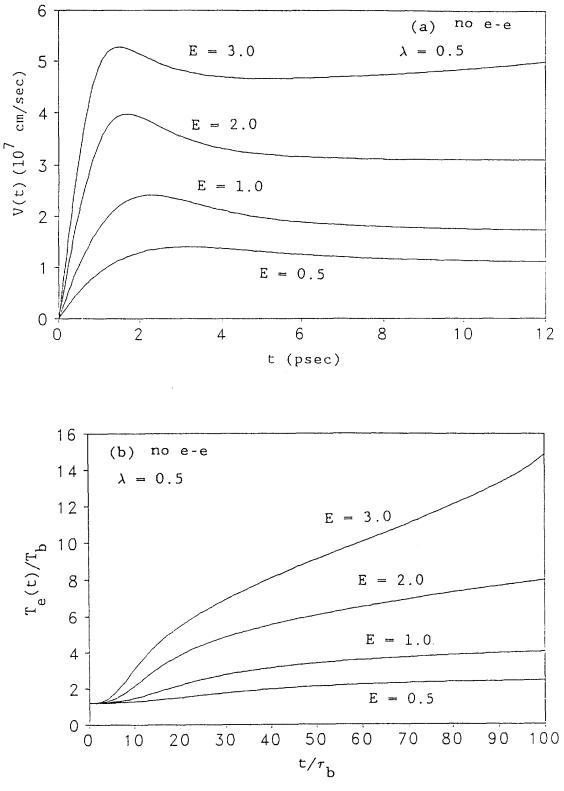

FIG. 3. (a) $V(t)$ vs t (picoseconds) for when e-e is not included. The different curves correspond to different applied electric-field values. (b) $T_e(t)/T_b$ vs t/τ_b with no e-e and different values of electric field.

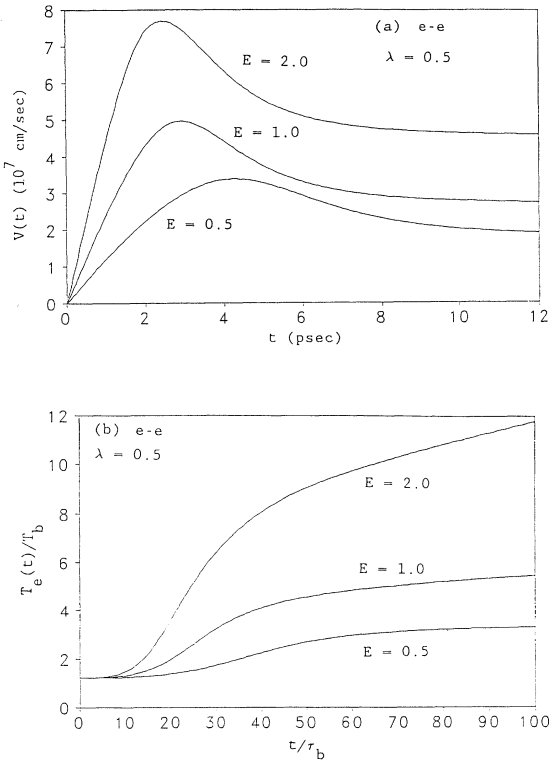

FIG. 4. (a) $V(t)$ vs t with e-e and different values of E. (b) $T_e(t)/T_b$ vs t/τ_b with e-e and different values of E.

the electron temperature may be too high for the present approximation to apply. We note that our overshoot value of $V(t)$ for $E=3$ kV/cm is about 1.6 times larger than the Monte Carlo value[19] for the screening parameter used here.

In Fig. 4 we show results similar to those of Fig. 3. We have included the e-e here. In Fig. 4(a) the velocity versus time curves have a similar behavior to those of Fig. 3(a). That is, the E field increases the overshoot and shifts it to shorter times. However, the magnitudes of the $V(t)$ as well as the T_e curves for the e-e case are greater in magnitude than those of Fig. 3 for no e-e. This difference is due to the decreased scattering rate and lower rate of energy loss of the electrons when the e-e interaction is included, as seen in Fig. 2.

Finally, concerning 2D and 3D transport, no attempt has been made in the present work to compare these two cases using the present approximation. In the work of Yokoyama and Hess,[19] however, the authors found that in the 2D case the velocity overshoot can be higher than it is in 3D for both 77 and 300 K. This suggests that perhaps the same is true for the electronic temperature T_e.

V. CONCLUSION

In this paper calculations have been carried out for the transient properties of electrons in a heterojunction interface in the presence of impurities and phonons. The hot-electron effects such as electron temperature and velocity overshoot as a function of applied electric field have been evaluated for electrons in the presence and absence of electron-electron interactions (e-e and no e-e).

In this work we have included screening effects on the ionized impurity in an approximate fashion. We have made use of a parameter λ through which value we include the screening. For $\lambda=0.5$ and $E=1$ kV/cm we have compared our calculation with a Monte Carlo method[19] for the case of no e-e and found a reasonable agreement for a reasonable field value; however, further work is needed to provide a much better comparison at much higher fields.

Here we have compared our calculations with Monte Carlo calculations to point out the differences between the two methods. It would be of great value to compare the transient velocity with experimental evidence when it becomes available. In particular, experimental electronic velocity and temperature at very short times would be most useful here.

The scattering mechanisms and energy-loss rates of electrons in the heterojunction interface have been calculated as a function of electron temperature. Both of these increase with T_e. The magnitudes of these two quantities are smaller for the case of when e-e is included than the case for which the e-e is not included. This difference is due to many-body screening effects.

The work carried out thus far is based on the simplest approximation for nonlinear electron transport equations obtained by Xing and Ting.[11] It would be of interest, however computationally involved, to study the full set of equations introduced in that work.

The effect of multisubband scattering that we found to be important[21] has not been investigated using the present nonlinear model. Further investigations to include multivalley effects are also needed.

ACKNOWLEDGMENTS

We would like to thank C. S. Ting for valuable discussions. One of us (J.H.) thanks L. M. Roth for encouraging conversations. He also thanks the members of code 3813 for their hospitality during his stay at NWC. We thank the NWC MSI fund for providing invaluable computer time. One of us (J.H.) was partly supported by the office of Naval Technology (ONT) as administered by the American Society of Engineering Education (ASEE). He was further supported by West Georgia College Faculty Research Grant No. 9213.

[1]R. Dingle, H. L. Stormer, A. C. Gossard, and W. Wiegman, Appl. Phys. Lett. **33**, 665 (1978).

[2]H. L. Stormer, A. Chang, D. C. Tsui, J. C. M. Hwang, A. C. Gossard, and W. Wiegmann, Phys. Rev. Lett. **50**, 1953 (1983).

[3]S. Hiyamizu, J. Saito, K. Nambu, and T. Ishikawa, Jpn. J. Appl. Phys. **22**, L609 (1983).

[4]J. Shah, IEEE J. Quantum Electron. **QE-22**, 1728 (1986).

[5]L. P. Kadanoff and G. Baym, *Quantum Statistical Mechanics* (Benjamin, New York, 1962); L. V. Keldysh, Zh. Eksp. Teor. Fiz. **47**, 1515 (1964) [Sov. Phys.—JETP **20**, 1018 (1965)]; K. K. Thornber and R. P. Feynmann, Phys. Rev. B **1**, 4099 (1970); V. P. Kalashnikov, Physica **48**, 93 (1970); J. R. Barker, in *Physics of Nonlinear Transport in Semiconductors,* edited by D. K. Ferry, J. R. Barker, and C. Jacoboni (Plenum, New York, 1980), pp. 126 and 589.

[6]E. M. Conwell, *High Field Transport in Semiconductors* (Academic, New York, 1967). See, for example, J. P. Nougier and M. Roland, Phys. Rev. B **8**, 5728 (1973); and more recently S. K. Sarker, *ibid.* **33**, 7263 (1986).

[7]C. Jacoboni and L. Reggiani, Rev. Mod. Phys. **55**, 645 (1983). See, for example, J. J. Maloney and J. Frey, J. Appl. Phys. **48**, 781 (1977); and more recently M. Tomizawa and K. Yokoyama, IEEE Electron. Dev. Lett. **EDL-5**, 464 (1984).

[8]X. L. Lei and C. S. Ting, Phys. Rev. B **36**, 8162 (1987).

[9]X. L. Lei and C. S. Ting, Phys. Rev. B **30**, 4809 (1984); **32**, 1113 (1985).

[10]C. S. Ting, S. C. Ying, and J. J. Quinn, Phys. Rev. B **14**, 4439 (1976).

[11]D. Y. Xing and C. S. Ting, Phys. Rev. B **35**, 3971 (1987).

[12]X. L. Lei, J. L. Birman, and C. S. Ting, Phys. Rev. B **58**, 2270 (1985).

[13]X. L. Lei, D. Y. Xing, M. Liu, C. S. Ting, and J. L. Birman, Phys. Rev. B **36**, 9134 (1987).

[14]H. Kroemer, Solid State Electron. **21**, 61 (1978); J. R. Barker

and D. K. Ferry, *ibid.* **23**, 519 (1980).
[15]F. Stern and W. E. Howard, Phys. Rev. **163**, 816 (1967).
[16]T. Ando, A. B. Fowler, and F. Stern, Rev. Mod. Phys. **54**, 437 (1982).
[17]J. Hasbun (unpublished).
[18]C. S. Ting and T. W. Nee, Phys. Rev. B **33**, 7056 (1986).
[19]K. Yokoyama and K. Hess, Phys. Rev. B **33**, 5595 (1986).
[20]X. L. Lei and C. S. Ting, Solid State Commun. **53**, 305 (1985).
[21]J. Hasbun and T. Nee (unpublished); J. Hasbun, Phys. Rev. B **43**, 5147 (1991).